Molecular Modeling Studies of the Akt PH Domain and Its Interaction with Phosphoinositides

Suo-Bao Rong,[†] Youhong Hu,[†] Istvan Enyedy,[†] Garth Powis,[‡] Emmanuelle J. Meuillet, Xiongwu Wu,[†] Renxiao Wang,[†] Shaomeng Wang,*[,†] and Alan P. Kozikowski*[,†]

Drug Discovery Program, Department of Neurology, Georgetown University Medical Center, 3970 Reservoir Road, Washington, D.C. 20007, and Arizona Cancer Center, 1515 North Campbell Avenue, Tucson, Arizona 85724

Received November 20, 2000

The serine−threonine protein kinase Akt is a direct downstream target of phosphatidylinositol 3-kinase (PI3-K). The PI3-K-generated phospholipids regulate Akt activity via directly binding to the Akt PH domain. The binding of PI3-K-generated phospholipids is critical to the relocalization of Akt to the plasma membrane, which plays an important role in the process of Akt activation. Activation of the PI3-K/Akt signaling pathway promotes cell survival. To elucidate the structural basis of the interaction of PI3-K-generated phospholipids with the Akt PH domain with the objective of carrying out structure-based drug design, we modeled the three-dimensional structure of the Akt PH domain. Comparative modeling-based methods were employed, and the modeled Akt structure was used in turn to construct structural models of Akt in complex with selected PI3-K-generated phospholipids using the computational docking approach. The model of the Akt PH domain consists of seven β-strands forming two antiparallel β-sheets capped by a C-terminal α-helix. The $\beta1-\beta2$, $\beta3-\beta4$, and $\beta6-\beta7$ loops form a positively charged pocket that can accommodate the PI3-K-generated phospholipids in a complementary fashion through specific hydrogen-bonding interactions. The residues Lys14, Arg25, Tyr38, Arg48, and Arg86 form the bottom of the binding pocket and specifically interact with the 3- and 4-phophate groups of the phospholipids, while residues Thr21 and Arg23 are situated at the wall of the binding pocket and bind to the 1-phosphate group. The predicted binding mode is consistent with known site-directed mutagenesis data, which reveal that mutation of these crucial residues leads to the loss of Akt activity. Moreover, our model can be used to predict the binding affinity of PI3-K-generated phospholipids and rationalize the specificity of the Akt PH domain for PI(3,4)P2, as opposed to other phospholipids such as PI(3)P and PI(3,4,5)P3. Taken together, our modeling studies provide an improved understanding of the molecular interactions present between the Akt PH domain and the PI3-K-generated phospholipids, thereby providing a solid structural basis for the design of novel, high-affinity ligands useful in modulating the activity of Akt.

Introduction

The serine−threonine protein kinase Akt [also called protein kinase B (PKB) or related to A- and C-kinase (RAC-PK)] is the downstream target of phosphatidylinositol 3-kinase (PI3-K).[1−4] PI3-K phosphorylates the 3-hydroxyl position of phosphatidylinositol (PI), phosphatidylinositol-4-phosphate [PI(4)P], and PI(4,5)P2 to produce PI(3)P, PI(3,4)P2, and PI(3,4,5)P3, respectively.[5,6] The PI3-K-generated phospholipids function as second messengers to regulate Akt activity[1,7,8] by directly binding to the pleckstrin homology (PH) domain of Akt.[9−11] The binding of PI3-K-generated phospholipids to the PH domain of Akt causes the translocation of Akt from the cytosol to the plasma membrane.[12−18] Translocation of Akt to the plasma membrane brings Akt in proximity to the membrane-bound protein kinase 3-phosphoinositide-dependent protein kinases 1 and 2 (PDK1 and 2) that phosphorylate and activate Akt.[2,19−23]

Akt plays an important role in the signaling network that controls cell growth. The upstream signal stemming from PI3-K is negatively regulated through dephosphorylation of the 3-position of the phosphoinositides by the tumor suppressor phosphatase−tensin homologue PTEN/MMAC,[24] mutations of which are frequently found in a number of human cancers.[25,26] Such mutations lead to elevated levels of PI(3,4,5)P3 and Akt activity.[27] Akt likely leads to enhanced cell survival through the phosphorylation of a number of downstream targets, including the pro- and anti-apoptotic Bcl-2 family member Bad,[28,29] the cell death pathway enzyme caspase-9,[30] and the glycogen synthase kinase 3 (GSK-3).[31,32] Activation of the PI3-K/Akt signaling pathway inhibits apoptosis in a variety of cancer cells and is crucial to promoting cell survival.[33−40] Thus, PI3-K and Akt represent novel targets for the discovery of drugs that may induce apoptosis in cancer cells in which Akt is overexpressed.

The PH domain is a structural module comprised of approximately 100 residues that has been identified in a large variety of proteins, many of which play a role in cellular signaling, cytoskeletal organization, or mediating protein−protein interactions that require association

* To whom correspondence and requests of reprints should be addressed. For A.P.K.: Tel: 202 687 0686. Fax: 202 687 5065. E-mail: kozikowa@giccs.georgetown.edu. For S.W.: Tel: 202 687 2028. Fax: 202 687 4032. E-mail: wangs@giccs.georgetown.edu.
[†] Georgetown University Medical Center.
[‡] Arizona Cancer Center.

10.1021/jm000493i CCC: $20.00
Published on Web 02/17/2001

Chart 1

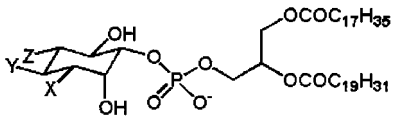

PI(3)P X = OPO_3^{2-}, Y = Z= H

PI(3,4)P2 X = Y = OPO_3^{2-}, Z= H

PI(3,4,5)P3 X = Y = Z = OPO_3^{2-}

with the cell membrane.[41,42] Although these PH domains lack primary sequence similarity, their three-dimensional (3D) structures are remarkably conserved.[42,43] PH domains specifically recognize and bind to phospholipids, which play a pivotal role in the regulation of intracellular signaling. Based upon the specificity of binding to phospholipids, PH domains can be grouped into three types, representatives of which are phospholipase C-δ (PLCδ), Bruton's tyrosine kinase (BTK), and Akt. The binding of the PLCδ PH domain to PI(4,5)-P2[44] is important for its targeting to the plasma membrane, and this leads to enhanced enzymatic activity[45] which can be inhibited by D-*myo*-inositol-1,4,5-trisphosphate [I(1,4,5)P3].[46] The PH domain of BTK binds to PI(1,3,4,5)P4 and PI(1,4,5)P3 with high affinity;[47,48] this binding interaction serves to translocate BTK to the plasma membrane, which thereby facilitates the phosphorylation and activation of BTK by the Src family tyrosine kinases.[20,21,49] The Akt PH domain specifically binds both PI(3,4)P2 and PI(3,4,5)P3 with comparable binding affinity, but only PI(3,4)P2 activates Akt.[9−11,50]

Although the structures of a number of PH domains have been determined by X-ray and NMR methods,[43] the structure of the Akt PH domain has not been determined by experiment. We were interested in gaining a better understanding of the structural basis of the selectivity and activation of Akt by certain PIPs and to use this information to carry out the structure-based design of ligands that might block Akt activation. Herein, we report our modeling studies of the 3D structure of the Akt PH domain and of the complexes formed between the modeled Akt PH domain and PI3-K-generated phospholipids.

Materials and Methods

Structure of PH Domain. The 3D structures of several PH domains have been determined by X-ray crystallography and NMR spectroscopy.[43] These studies reveal that the PH domains from β-spectrin, pleckstrin, dynamin, PLCδ, and BTK are very similar.[51−55] The core structure of the PH domains is composed primarily of seven β-strands, which form two antiparallel β-sheets, together with a C-terminal α-helix. The loops linking the neighboring β-strands, particularly the $\beta1-\beta2$, $\beta3-\beta4$, and $\beta6-\beta7$ loops, are variable in length and in sequence. These loops are located at the opposite surface of the C-terminal α-helix and form the phospholipid-binding pocket.

Homology Modeling. The sequence alignment of PH domains was retrieved from the protein family database of alignment.[56−58] The secondary structural information obtained from the consensus prediction method,[59,60] and the Protein Data Bank (PDB) summary database[61] for the sequences and structures of the PH domains was used to adjust the sequence alignment, since the accuracy of the modeled structure is greatly dependent on the quality of the sequence alignment. The final sequence alignment was checked using the structure−structure alignment taken from the FSSP database.[62,63]

Modeling was carried out on a Silicon Graphics Indigo2/IMPACT 10000 workstation using the InsightII and Discover programs (Molecular Simulation, Inc., San Diego, CA). The core structure of the Akt PH domain was modeled based on the sequence alignment using the crystal structure of BTK (PDB entry 1BWN)[64] as the template. Amino acid substitutions were built using a side chain rotamer library. Deletions and insertions were constructed by means of the loop database search.[65,66] The initial model was refined in a stepwise manner by energy minimization using the Amber force field.[67,68] First, the loops were refined with 500 steps of minimization with a fixed and a free backbone, respectively. Then, all side chains with a constrained backbone were minimized for 500 steps, followed by another 2000 steps of minimization for the whole model. The final model was checked for its quality using the program PROCHECK.[69] The electrostatic potential of the model of the Akt PH domain was calculated with the program Delphi implemented in InsightII.

Docking. The structures of PI(3)P, PI(3,4)P2, and PI(3,4,5)-P3 were constructed using the structure of Ins(1,3,4,5)P4 extracted from the crystal structure of BTK (1BWN.pdb) in complex with this inositol phosphate. As our present modeling studies focus only on the interaction of the PIPs with the PH domain of Akt and do not consider the interaction of their lipid fragments with the membrane, the lipid chains of the modeled PIPs were shortened to $-OPO_3CH_2CH(OCOC_2H_5)CH_2OCOC_2H_5$.

Computational docking was performed using a flexible docking method FlexX.[70] First, the known protein−ligand complexes of PH domains taken from the PDB,[71] including 1BWN.pdb[64] and 1MAI.pdb,[54] were employed to validate the quality of the PH domain−phospholipid complex achieved by the FlexX program. Then, the PI3-K-genrated phospholipids PI(3)P, PI(3,4)P2, and PI(3,4,5)P3 were docked sequentially into the positively charged pocket formed by the $\beta1-\beta2$, $\beta3-\beta4$, and $\beta6-\beta7$ loops of the model of the Akt PH domain.

The conjugate algorithm, implemented in the InsightII/Discover program, was used in the energy minimization. The complex models of PI(3)P, PI(3,4)P2, and PI(3,4,5)P3 were energetically minimized for 5000 steps or until an energy gradient of less than 0.005 kcal·mol^{-1}·Å^{-1} was achieved. The complex structures were then solvated with a 10 Å water sphere, and the same minimization was performed.

Analysis of the Hydrogen-Bonding Interactions. Hydrogen-bonding interactions play a pivotal role in the binding of the inositol analogues to the PH domains, as revealed by the available X-ray crystal structures.[51−55,64] A hydrogen bond involves four atoms: D, H, A, and AA (donor, hydrogen, acceptor, and acceptor antecedent), and its strength depends on both the nature of the donor and acceptor atoms and the geometrical parameters such as the distance r_{DA} and the angles θ_{D-H-A} and θ_{H-A-AA}. The molecular dynamics (MD) simulation was used to examine the hydrogen-bonding interactions of the Akt PH domain with the PI3-K-generated phospholipids.

The MD simulations were performed on a Beowulf cluster with 450-MHz Pentium III CPU processors, using a standalone version of the CHARMM program,[72] version c27b2, and the all-atom version 22 force field.[73,74] The energetically minimized models of the Akt PH domains in complex with PI(3)P, PI(3,4)P2, and PI(3,4,5)P3 were used as the starting structures in the MD simulations. The MD simulation was carried out with a 5-ps heating period, a 100-ps equilibration, and a 200-ps constant temperature simulation at 300 K with a step size of 0.001 ps. Trajectories were recorded every 0.1 ps during the simulations. A shake algorithm was used to constrain all bonds involving hydrogens.[75]

Upon the basis of the trajectories of the MD simulations, we examined the hydrogen-bonding interactions dynamically and measured the distance r_{DA} and the angles θ_{D-H-A} and θ_{H-A-AA} as well as the hydrogen-bonding energy.

Prediction of Binding Affinities. To further examine the quality of the models of the Akt PH domain in complex with PI3-K-generated phospholipids, the empirical approaches

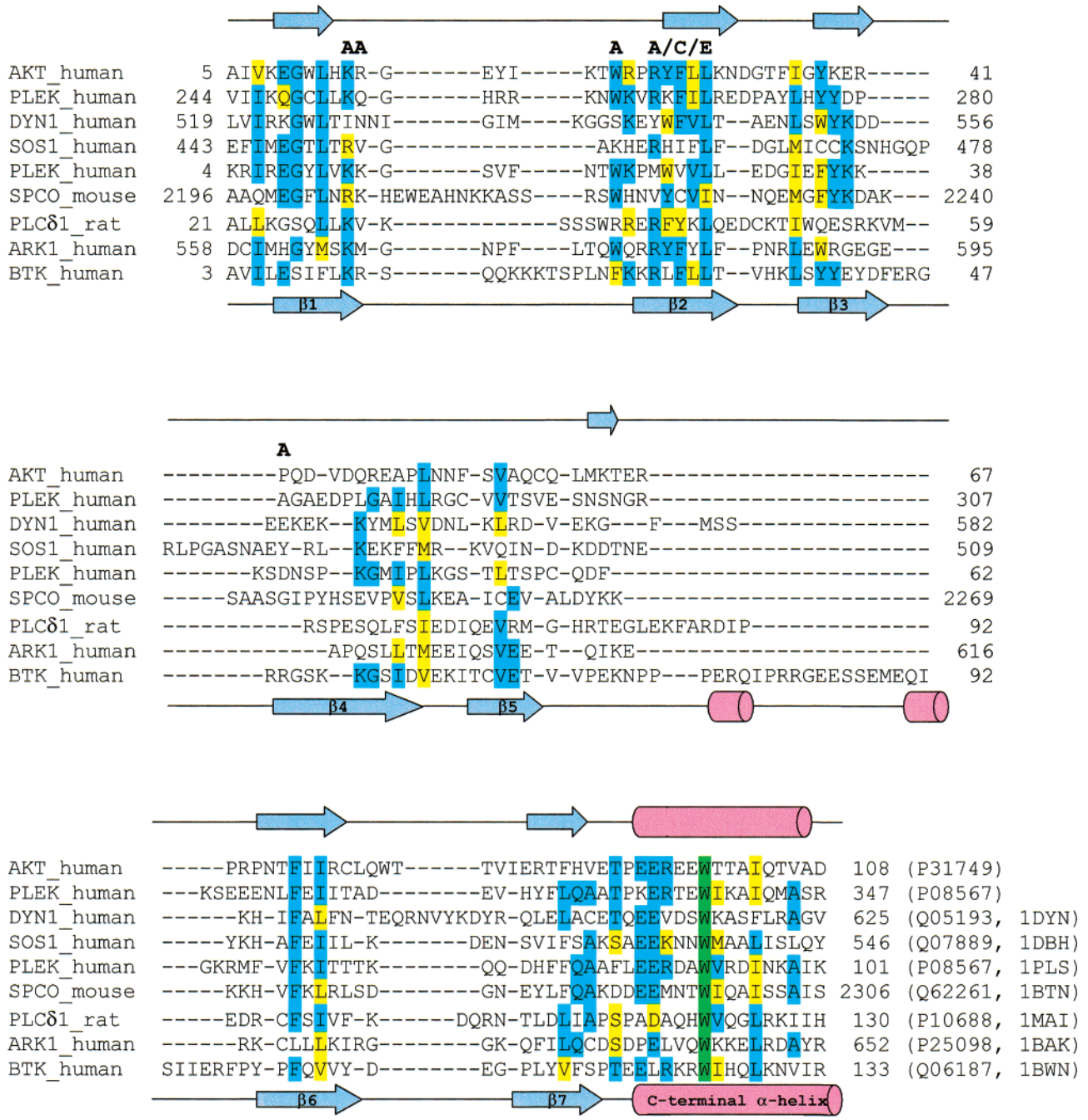

Figure 1. Sequence alignment of PH domains. The SWISS-PROT accession numbers or PDB entries are indicated at the end of the sequences. Secondary structure information of the Akt PH domain and the template protein, BTK_human, are shown above and below the sequence alignment, respectively. The Akt activity-abolishing mutations (K14A, R15A, W22A, R25A/C/E, and P42A) are indicated at the top of the sequence alignment.

SCORE[76] and ChemScore[77] were employed to estimate the binding affinities of PI3-K-generated phospholipids to the Akt PH domain.

Results and Discussion

Sequence Alignment. Because the PH domains share only limited sequence similarity, the general methods of sequence search and sequence alignment, such as ClustalW and Blast,[78−82] cannot be used to obtain an accurate sequence alignment for these PH domains. Therefore, the protein family database was employed to retrieve the sequence alignment of the Akt PH domain with other known PH domains. The protein family database is a database of multiple sequence alignment of protein domain families which is organized based upon their hidden Markov model profiles.[56−58] From the protein family database, the sequence alignment was retrieved for more than 150 PH domains. After making adjustments based upon secondary structure information with further checks being made by structure−structure alignment (FSSP database), the required sequence alignment was selected for modeling of the Akt PH domain (Figure 1).

Although PH domains have only limited sequence similarity, multiple sequence alignment shows that these PH domains have seven common blocks of ungapped segments, which respectively correspond to

seven secondary structural segments of the template protein: β1, β2, β3, β4, β5, β6, and (β7 + α). In addition, the predicted secondary structure elements of the Akt PH domain are distributed similarly to those of the template protein (Figure 1). Specifically, the aligned sequences share a similar distribution of charged and hydrophobic residues. From a comparison of the alignment of all 164 seed sequences in the protein family database,[58] the aligned sequences have five strikingly conserved residues including three aromatic residues (tryptophan in block 2 and two phenylalanines in block 7), one basic residue (arginine in block 4), as well as one hydrophobic residue (leucine in block 7). All of these features in multiple sequence alignment reflect the structural conservation of the PH domains at the level of the amino acid sequence. Accordingly, this sequence alignment (Figure 1) can be employed to model the structure of the Akt PH domain.

An examination of the PDB reveals that there are only three structures available of a PH domain in complex with an inositol phosphate. Two of these are the PH domains of spectrin β (1BTN.pdb) and PLCδ1 (1MAI.pdb) in complex with D-*myo*-inositol-1,4,5-triphosphate; the third is the BTK PH domain in complex with inositol-1,3,4,5-tetrakisphosphate (1BWN.pdb and 1B55.pdb). BTK, as well as Akt, functions downstream of PI3-K which generates the phospholipids necessary for their activation.[12,20,21,49] The N-terminus of the Akt PH domain is essential for PI(3,4)P2-mediated stimulation,[50] while the N-terminus of the BTK PH domain plays a key role in the binding of PI(3,4,5)P3.[64] Furthermore, the Akt activity-abolishing mutations localized at the N-terminus of the Akt PH domain, Lys14Ala, Trp22Ala, and Arg25Ala/Cys/Glu,[10,14,83] are homologous with the X-linked agammaglobulinemia-causing mutations of the BTK PH domain, Lys12Arg, Phe25Ser, and Arg28Cys/His/Pro, respectively.[84] Thus, the crystal structure of the BTK PH domain (1BWN.pdb) was used as the template for modeling the Akt PH domain.

The Akt PH domain, in comparison to the template protein, has two insertions of 2 and 3 residues, as well as three deletions of 5, 5, and 24 residues. All of the insertions and deletions are localized to the loops connecting the neighboring secondary structure elements.

Structural Model of the Akt PH Domain. The model of the Akt PH domain, showing an acceptable Ramanchandran plot and other stereochemical parameters under protein structure verification, consists of seven β-strands and a C-terminal α-helix (Figure 2), each of which corresponds to one sequence block, respectively (Figure 1). The core structure of the model of the Akt PH domain is composed of an antiparallel β-sandwich of two sheets, one end of which is capped by the C-terminal α-helix. In the sandwich, the N-terminal half of the Akt PH domain forms a four-stranded antiparallel β-sheet that packs almost orthogonally against the second β-sheet of three strands (Figure 2). Hydrophobic side chains from both the β-sheets project into the center of the domain to generate the hydrophobic core.

The surface electrostatic potential shows that the model of the Akt PH domain is electrostatically polarized (Figure 2). The β1−β2, β3−β4, and β6−β7 loops form a positively charged face on one side of the domain, while the opposite face, containing the C-terminal α-helix, is negatively charged.

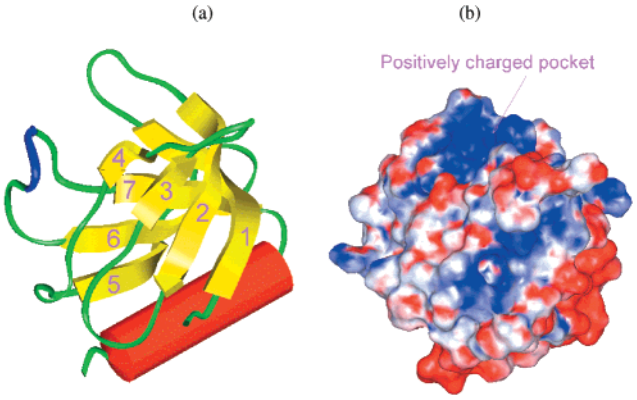

Figure 2. Structural model of the Akt PH domain. (a) Schematic drawing of the model. The β-strands, α-helix, turn, and coils are shown as the yellow arrow, red cylinder, blue ribbon, and green ribbon, respectively. (b) Electrostatic surface of the model with the same view as in panel a. Negative potential is shown in red, positive potential in blue. One positively charged pocket is formed by the β1−β2, β3−β4, and β6−β7 loops.

Docking. The FlexX is a fast docking program for predicting protein−ligand interactions,[70] in which the placement algorithm of the base fragment was employed.

As described in the Introduction, based upon the specificity of binding to phospholipids, PH domains can be divided into three groups. Their representatives include the BTK PH domain in complex with PI(1,3,4,5)-P4 (1BWN.pdb) and the PLCδ PH domain in complex with PI(4,5)P2 (1MAI.pdb) as determined by X-ray crystallography, as well as the Akt PH domain which binds PI(3,4)P2. To examine the accuracy of the interaction of the PH domain with phospholipids predicted by the FlexX program, the crystal structures of the BTK PH domain in complex with PI(1,3,4,5)P4 (1BWN.pdb) and the PLCδ PH domain in complex with PI(1,4,5)P3 (1MAI.pdb) were used to perform the docking test. The results are presented in Table 1.

The experimentally observed structures of the BTK PH domain in complex with PI(1,3,4,5)P4 and the PLCδ PH domain in complex with PI(1,4,5)P3 are reproduced by the docking test with 1.3 and 1.1 Å rms deviation. Most importantly, the interaction mode revealed by the crystal structures is almost identical to that predicted by the FlexX program. For the BTK PH domain in complex with PI(1,3,4,5)P4, the crystal structure revealed that the hydrogen bond networks are formed between the 1-, 3-, 4-, and 5-phosphate groups and the eight residues Lys12, Gln15, Lys17, Lys18, Ser21, Asn24, Arg28, and Tyr39. These hydrogen bond networks are approximately reproduced by the FlexX docking test with only two exceptions: Gln16 and Asn24 (Table 1). The experimentally observed hydrogen bond interactions in the crystal structure of the PLCδ PH domain in complex with PI(1,4,5)P3 are also reproduced by the FlexX program except for one binding residue: Ser55 (Table 1). Thus, our results suggest that the FlexX program may be used to predict the interaction mode of PI3-K-generated phospholipids with the model of the Akt PH domain.

Table 1. Comparison of Hydrogen Bond Interactions Predicted by FlexX and Retrieved from Crystal Structures.

		hydrogen bond interactions			
PDB	rms (Å)	predicted by FlexX		X-ray structure	
1BWN	1.342	Lys12	1 HB with 3-PG[a]	Lys12	2 HBs with 3-PG
			1 HB with 4-PG		1 HB with 4-PG
		Gln15	1 HB with 4-PG	Gln15	1 HB with 4-PG
		Gln16	1 HB with 5-PG		
				Lys17	2 HBs with 5-PG
		Lys18	1 HB with 5-PG	Lys18	1 HB with 5-PG
		Ser21	2 HBs with 5-PG	Ser21	1 HB with 5-PG
				Asn24	1 HB with 1-PG
		Arg28	1 HB with 3-PG	Arg28	2 HBs with 3-PG
		Tyr39	1 HB with 4-PG	Tyr39	1 HB with 4-PG
1MAI	1.144	Lys30	1 HB with 4-PG	Lys30	2 HBs with 4-PG
					1 HB with 5-PG
		Lys32	1 HB with 4-PG	Lys32	1 HB with 4-PG
		Trp36	1 HB with 1-PG	Trp36	1 HB with 1-PG
		Arg40	2 HBs with 5-PG	Arg40	2 HBs with 5-PG
				Ser55	1 HB with 5-PG
		Arg56	1 HB with 5-PG	Arg56	1 HB with 5-PG
		Lys57	1 HB with 4-PG	Lys57	1 HB with 4-PG
			1 HB with 5-PG		2 HBs with 5-PG

[a] HB and PG represent hydrogen bond and phosphate group, respectively.

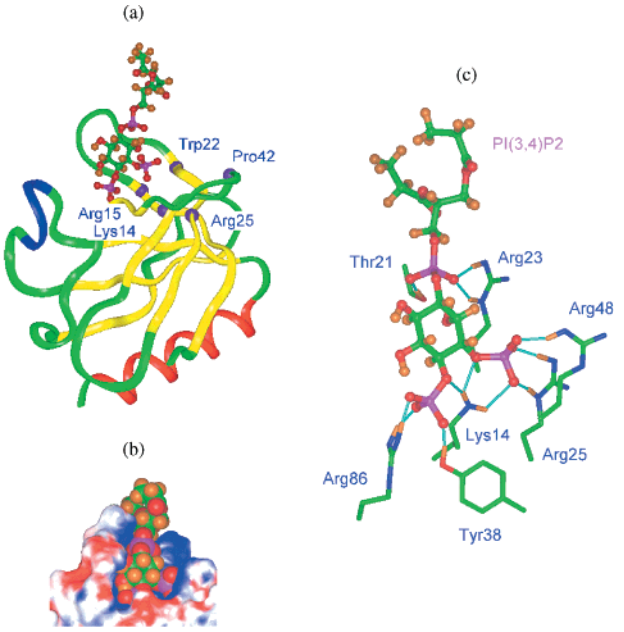

Figure 3. Complex model between the Akt PH domain and PI(3,4)P2. The lipid chain of PI(3,4)P2 was truncated to $-OPO_3CH_2CH(OCOC_2H_5)CH_2OCOC_2H_5$ as described in context. (a) Shown in the same orientation as in Figure 1. PI(3,4)P2 is located among the $\beta1-\beta2$, $\beta3-\beta4$, and $\beta6-\beta7$ loops. The residues of Akt-abolishing mutations are displayed by α-carbon atoms. (b) View is rotated −45° along the *y* axis of panel a. The PI(3,4)P2 molecule is placed in the positively charged binding pocket in a complementary fashion. (c) View is rotated −60° along the *y* axis of panel a. The 3,4-phosphate groups are anchored via hydrogen bonds with Lys14, Arg25, Tyr38, Arg48, and Arg88. The 1-phosphate group forms hydrogen-bonding interactions with Thr21 and Arg23.

Complex Models and Ligand−Akt Interaction. In the complex models of the Akt PH domain with PI3-K-generated phospholipids, the ligands are situated in a complementary fashion within the positively charged pocket surrounded by the $\beta1-\beta2$, $\beta3-\beta4$, and $\beta6-\beta7$ loops (Figure 3). In the positively charged pocket, the phospholipid-binding site is comprised mainly of seven residues, including Lys14, Thr21, Arg23, Arg25, Tyr38, Arg48, and Arg86. In the model of the Akt PH domain, these phospholipid-binding residues, Lys14, Thr21, Arg23, Arg25, Tyr38, Arg48, and Arg86, are sequentially distributed at the end of $\beta1$, the end of the $\beta1-\beta2$ loop, the beginning of $\beta2$, the middle of $\beta2$, the middle of $\beta3$, the middle of $\beta4$, and the beginning of $\beta7$. Most of the interactions are charge−charge interactions with hydrogen bonding between the phosphate groups and the positively charged amino acid residues.

In the complex model of the Akt PH domain with PI(3,4)P2 and PI(3,4,5)P3, there exist two sets of hydrogen bond networks. The first set is formed between the 3- and 4-phosphate groups and the residues Lys14, Arg25, Tyr38, Arg48, and Arg86. Although these residues originate from different β-strands, the conformation of their side chains is able to accommodate the conformation of the 3- and 4-phosphate groups. All of these 3- and 4-phosphate-binding residues form a "claw" at the bottom of the binding pocket to capture the 3- and 4-phosphate groups through eight hydrogen bonds. Thus, this hydrogen bond network may play an important role in the recognition of appropriate phospholipids by the PH domain. The second set of hydrogen-bonding networks is formed between the 1-phosphate group and residues Thr21 and Arg23. Thr21 forms one hydrogen bond with the 1-phosphate group, while Arg23 interacts with the 1-phosphate group through two hydrogen bonds. The 1-phosphate-binding residues, Thr21 and Arg23, form a "pincer" at the wall of the binding pocket to fix the orientation of the phospholipids. Therefore, this second hydrogen bond network is likely to direct the orientation of the lipid portion of the phospholipid.

Analysis of Hydrogen-Binding Interactions. Because the hydrogen bond interactions between the 1-phosphate group and the "pincer" residues situated at the wall of binding pocket are very similar among the phospholipids PI(3)P, PI(3,4)P2, and PI(3,4,5)P3, our analysis of the hydrogen bond interactions focuses only on the "claw" residues located at the bottom of binding pocket, which include Lys14, Arg25, Tyr38, Arg48, and Arg86. Based upon the MD trajectories of the 3D structural models, the averaged distance r_{DA} and the angles θ_{D-H-A} and θ_{H-A-AA}, as well as hydrogen-bonding energies, were calculated for the Akt PH domain in complex with PI(3)P, PI(3,4)P2, and PI(3,4,5)P3. These data are shown in Table 2.

Comparison of the complex models between the PI3-K-generated phospholipids and the Akt PH domain as well as their estimated hydrogen-bonding energies shows that the 3- and 4-phosphate groups of PI(3,4)P2 and PI(3,4,5)P3 interact with the Akt PH domain through eight hydrogen bonds in a similar fashion. The 3-phosphate group forms five hydrogen bonds: two with the two amide hydrogen atoms of the side chain of Lys14, two with the amide hydrogen and ϵ-amide hydrogen of the side chain of Arg25, and the other with the amide hydrogen of the side chain of Arg48. The hydrogen bond energies (Table 2) show that, among these five hydrogen bonds, three hydrogen bonds with Arg25 and Arg48 have more negative hydrogen bond energies ($E_{HB} \sim -3.3$ kcal/mol) and smaller fluctuation (deviation of $E_{HB} \sim 0.1-0.3$ kcal/mol). Obviously, the three hydrogen bonds stemming from the interactions of the 3-phosphate group with Arg25 and Arg48 are

Table 2. Hydrogen-Bonding Energies Calculated Based Upon the MD Trajectories

compd	donor	acceptor	r_{DA} (Å)	θ_{D-H-A} (deg)	θ_{A-H-AA} (deg)	E_{HB} (kcal/mol)
PI(3,4,5)P3	NH (side chain, Arg25)	$O1_{(3-PG)}$[a]	2.77 ± 0.10	146.0 ± 9.4	121.9 ± 9.8	−3.31 ± 0.10[b]
	NH1 (side chain, Lys14)	$O2_{(3-PG)}$	3.99 ± 0.16	90.1 ± 11.4	63.5 ± 4.2	−1.87 ± 0.28
	NHE (side chain, Arg25)	$O2_{(3-PG)}$	2.76 ± 0.10	126.8 ± 9.8	86.53 ± 4.2	−3.28 ± 0.22
	NH2 (side chain, Lys14)	$O3_{(3-PG)}$	2.47 ± 0.08	108.6 ± 10.5	86.8 ± 4.8	−1.49 ± 0.92
	NH (side chain, Arg48)	$O4_{(3-PG)}$	2.77 ± 0.13	118.6 ± 15.2	127.2 ± 7.3	−3.26 ± 0.28
	NH1 (side chain, Arg86)	$O1_{(4-PG)}$	3.11 ± 0.20	121.4 ± 13.5	86.0 ± 8.8	−3.26 ± 0.26
	OH (side chain, Tyr38)	$O2_{(4-PG)}$	3.70 ± 0.32	130.5 ± 13.9	76.4 ± 14.5	−2.48 ± 0.63
	NH2 (side chain, Arg86)	$O3_{(4-PG)}$	2.76 ± 0.10	141.6 ± 9.3	85.1 ± 13.2	−3.28 ± 0.22
total						−22.23
PI(3,4)P2	NH (side chain, Arg25)	$O1_{(3-PG)}$	2.64 ± 0.08	139.6 ± 11.6	132.2 ± 16.2	−2.92 ± 0.36
	NH1 (side chain, Lys14)	$O2_{(3-PG)}$	4.33 ± 0.20	99.6 ± 24.3	43.7 ± 3.8	−1.14 ± 0.46
	NHE (side chain, Arg25)	$O2_{(3-PG)}$	3.00 ± 0.19	151.0 ± 10.6	151.0 ± 10.6	−3.36 ± 0.22
	NH2 (side chain, Lys14)	$O3_{(3-PG)}$	3.81 ± 0.18	56.3 ± 32.0	70.4 ± 8.5	−2.17 ± 0.29
	NH (side chain, Arg48)	$O4_{(3-PG)}$	2.90 ± 0.18	116.0 ± 14.1	137.6 ± 9.3	−3.35 ± 0.20
	NH (side chain, Arg86)	$O1_{(4-PG)}$	3.14 ± 0.32	134.9 ± 12.7	131.8 ± 10.2	−3.13 ± 0.40
	OH (side chain, Tyr38)	$O2_{(4-PG)}$	4.02 ± 0.67	68.9 ± 48.2	101.9 ± 19.4	−1.80 ± 1.37
	NH (side chain, Arg86)	$O3_{(4-PG)}$	2.70 ± 0.09	133.2 ± 17.1	102.3 ± 13.5	−3.11 ± 0.34
total						−20.98
PI(3)P	NH (side chain, Arg25)	$O1_{(3-PG)}$	2.82 ± 0.15	137.7 ± 9.6	85.2 ± 5.2	−3.33 ± 0.21
	NH1 (side chain, Lys14)	$O2_{(3-PG)}$	5.01 ± 0.35	50.5 ± 5.0	81.8 ± 6.8	−0.17 ± 0.37
	NHE (side chain, Arg25)	$O2_{(3-PG)}$	2.86 ± 0.10	138.6 ± 8.5	148.4 ± 10.6	−3.44 ± 0.09
	NH (side chain, Arg48)	$O3_{(3-PG)}$	3.44 ± 0.33	67.3 ± 7.2	70.2 ± 5.4	−3.12 ± 0.33
total						−10.06

[a] PG represents phosphate group. [b] Average value ± standard deviation.

stronger and more stable than other two hydrogen bonds originating from Lys14 (Table 2). The 4-phosphate group forms three hydrogen bonds: one with the hydroxyl hydrogen of Tyr38 and the other two from the two amide hydrogen atoms of the side chain of Arg86. Comparison of these reveals that the two hydrogen bonds with Arg86 are stronger and more stable than the one from Tyr38. Although the PI(3,4)P2 and PI(3,4,5)P3 interact with the Akt PH domain in a similar fashion, the location of PI(3,4,5)P3 within the binding pocket as well as the orientation of its lipid portion is obviously affected by the presence of the 5-phosphate group.

In contrast to PI(3,4)P2 and PI(3,4,5)P3, PI(3)P has only one phosphate group that could interact with the binding residues located at the bottom of binding pocket. The complex model and the predicted binding affinity reveal that only four hydrogen bonds are formed with the residues Lys14, Arg25, and Arg48. Thus, the binding of PI(3)P to the Akt PH domain is relatively weak.

Previous site-directed mutagenesis studies showed that the mutations, Lys14Ala, Trp22Ala, and Arg25Ala/Cys/Glu, abolish the activity of Akt.[83] The predicted interaction mode is consistent with these mutation data, as such mutations would be expected to substantially reduce the strength of the PH domain−phosphate interactions. The mutations Lys14Ala and Arg25Ala/Cys/Glu result in the loss of four hydrogen bonds to the 3-phosphate group. The mutation Trp22Ala would affect the orientation of the side chains of Thr21 and Arg23, thereby weakening the interactions of Thr21 and Arg23 with the 1-phosphate group and thus influencing the orientation of the lipid portion of the phospholipids.

Some mutagenesis of the non-phospholipid-binding residues located on the $\beta1-\beta2$ and $\beta3-\beta4$ loops revealed that the $\beta1-\beta2$ and $\beta3-\beta4$ loops interact substantially with the negatively charged phospholipid headgroup region of the membrane.[64,85−87] For example, the mutation Glu41Lys on the BTK PH domain results in constitutive activation of BTK, probably because the positively charged Lys which substitutes Glu41 is beneficial to the association of the BTK PH domain to membrane.[88] The Glu54Lys mutation of the PLCδ PH domain leads to a similar gain in protein function.[85] In the model of the Akt PH domain in complex with PI(3,4,5)P3, the negatively charged 5-phosphate group of PI(3,4,5)P3 extends outside and proximal to the $\beta1-\beta2$ loops. This exposed negatively charged phosphate group is likely to be unfavorable to the binding of the Akt PH domain to the phospholipid bilayer, which may explain why PI(3,4,5)P3 fails to activate Akt although it binds to the Akt PH domain with an affinity similar to that of PI(3,4)P2.

Specificity of the Akt PH Domain. In comparison to the structure of the BTK PH domain, the $\beta1-\beta2$ and $\beta3-\beta4$ loops of the Akt PH domain are shorter and the $\beta6-\beta7$ loop is longer (Figure 4). The $\beta1-\beta2$ loop of the BTK PH domain contains three 5-phosphate-binding residues (Lys17, Lys18, and Ser21), whereas no residues on the shorter $\beta1-\beta2$ loop of the Akt PH domain are available to interact strongly with the 5-phosphate group. Although there exist three potential hydrogen bond-forming residues (Arg15, Tyr18, and Lys20), their side chains are all directed outside of the binding pocket, and thus they cannot contribute to ligand binding. The sequence alignment and the 3D structures of the Akt and BTK PH domains show that some 3- and 4-phosphate-binding residues are located at conserved positions. For example, the 3- and 4-phosphate-binding residues of the Akt PH domain, namely Arg14, Arg25, and Tyr38, correspond respectively to Lys12, Arg28, and Tyr39 of the BTK PH domain. In the Akt PH domain, there are two other nonconserved 3- and 4-phosphate-binding residues, Arg48 and Arg86, which alter the orientation of PI(3,4)P2 bound to the Akt PH domain from that of Ins(1,3,4,5)P4 bound to the BTK PH domain (Figure 4).

In contrast to the Akt PH domain, the PLCδ1 PH domain has the shorter $\beta1-\beta2$, $\beta3-\beta4$, and $\beta6-\beta7$ loops. The $\beta3-\beta4$ loop of the PLCδ1 PH domain is not

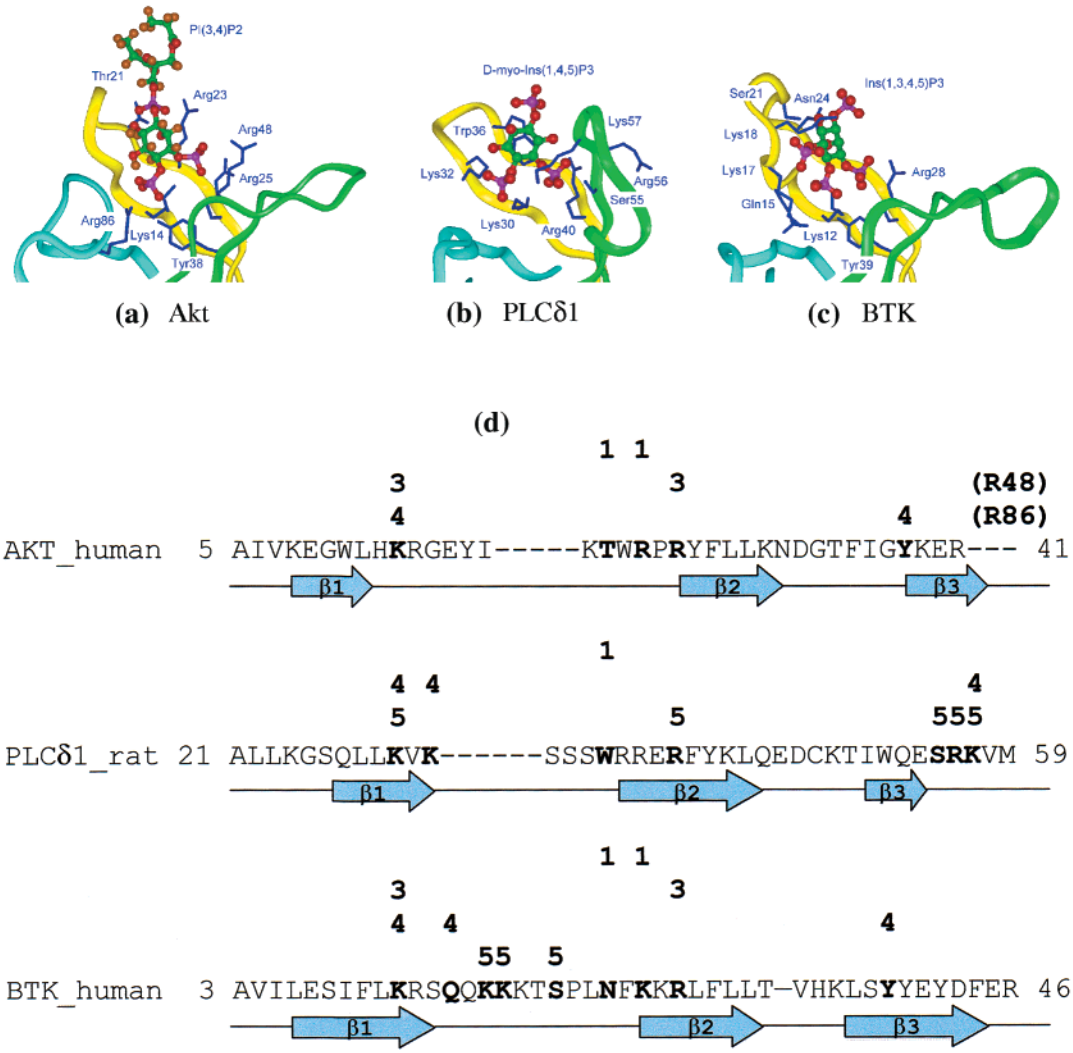

Figure 4. Binding sites and specificity of PH domain. (a) Interactions between the Akt PH domain and PI(3,4)P2. (b) Interactions between the PLCδ1 PH domain and D-*myo*-inositol-1,4,5-triphosphate [D-*myo*-Ins(1,4,5)P3]. (c) Interaction between the BTK PH domain and inositol-1,3,4,5-tetrakisphosphate [Ins(1,3,4,5)P4]. The β1−β2, β3−β4, and β6−β7 loops are yellow, green, and light blue, respectively. (d) Sequence alignment of the beginning three β-strands of the Akt, PLCδ1, and BTK PH domains extracted from Figure 1. The residues contributing to phospholipid-binding specificity are indicated by the position number of the phosphate groups at the top of the sequences. The secondary structures are shown at the bottom of the sequences.

extended and is closer to the β1−β2 loop. It is interesting to note that the 5-phosphate-binding residues are contributed mainly by the β3−β4 loop, whereas the 4-phosphate-binding residues originate primarily from the β1−β2 loop. Thus, the orientation of D-*myo*-Ins-(1,4,5)P3 complexed with the PLCδ1 PH domain is quite different from that of PI(3,4)P2 complexed with the Akt PH domain (Figure 4).

Akt Activity-Abolishing Mutations. Site-directed mutagenesis studies have shown that four mutations of Lys14Ala, Arg15Ala, Trp22Ala, and Arg25Ala/Cys/Glu abolish the activity of Akt.[10,14,83] In the model of the Akt PH domain, these four Akt activity-abolishing mutations appear at the positively charged phospholipid-binding pocket.

The two residues Lys14 and Arg25 are situated at the bottom of the positively charged pocket (Figure 3), and their side chains can directly interact with the 3- and 4-phosphate groups borne by the phospholipids. According to the predicted interaction mode, the mutations of Lys14Ala and Arg25Ala/Cys/Glu could lead to the loss of four hydrogen bonds between Lys14 and Arg25 with the 3-phosphate groups. Thus, the Akt mutants of Lys14Ala and Arg25Ala/Cys/Glu do not bind PI3-K-generated phospholipids, probably as a consequence of the loss of these two important, positively charged binding residues at the bottom of phospholipid-binding pocket. The side chains of the residues Arg15 and Trp22 are directed to the outside of the Akt PH domain, although they are close to the phospholipid-binding pocket (Figure 3). The Arg15 situated at the end of β-strand 1, in the model of the Akt PH domain, forms a salt bridge with Glu64 located at the middle of the β5−β6 loop (Figures 3 and 4); hence, the mutation of Arg15 to Ala could induce a substantial change in local structure due to the loss of this salt bridge. Trp22 is located between the 1-phosphate-binding residues Thr21 and Arg23. Specifically, this residue is situated at the beginning of β-strand 2. In the model of the Akt PH domain, β-strand 2, together with β-strand 1, bends at the middle and thus is crucial for maintaining the core structure of the Akt PH domain, i.e., the antiparallel β-sheet structure. When Trp22 is substituted by a small amino acid (Ala), the beginning of β-strand 2 could

become more flexible so that the local conformation would be disturbed to some extent. On the other hand, the mutation Trp22Ala could also influence the conformation of the side chains of Thr21 and Arg23 so that the interaction with the 1-phosphate group is weakened.

In addition to the above four Akt activity-abolishing mutations, there are four other mutations that have been made to the Akt PH domain: Lys39Ala, Glu40Ala/Cys/Lys, Arg41Ala, and Pro42Ala. All of the Glu40 mutations resulted in a slightly enhanced Akt activity, whereas the mutation Pro42Ala markedly reduced Akt activity. The Lys39Ala and Arg41Ala mutants showed normal Akt activity. In the model of the Akt PH domain, all of these mutated residues are situated from the beginning to the top of the $\beta3-\beta4$ loop. The side chain of Glu40 is directed to the phospholipid-binding pocket although Glu40 is not a phospholipid-binding residue. When this negatively charged residue is substituted by the positively charged residue Lys or by the neutral residues Ala and Cys, the phospholipid-binding pocket would become relatively more positive. This change would presumably be beneficial for the recognition and binding of phospholipids to the Akt PH domain. The mutation Pro42Ala, located at the top of the $\beta3-\beta4$ loop, is remote from the phospholipid-binding pocket. However, Pro is a highly constrained residue that is involved in maintaining protein structure. Therefore, the mutation Pro42Ala may greatly influence, or possibly even break, the loop linking the $\beta3$- and $\beta4$-strands so that the binding pocket conformation is greatly altered, leading to the reduced ability of Akt to bind its phospholipids. Although the mutations Lys39Ala and Arg41 could increase the flexibility at the beginning of the $\beta3-\beta4$ loop, the interaction of the Akt PH domain with phospholipids would not be disturbed by these two mutations, since these residues Lys39 and Arg41 do not contribute to the phospholipid-binding pocket and their side chains are oriented to the outside of the Akt PH domain.

Comparison of Our Model with a Previously Published Model of the Akt PH Domain. The Akt PH domain was first modeled in 1998 when Tsichlis's group studied the mutagenesis and the activation mechanism of the Akt PH domain.[83] Their model is based upon a hybrid structural template derived from PLCδ and the pleckstrin N-terminal PH domains. These two PH domains specifically bind to PI(4,5)P2,[89,90] whereas the Akt PH domain binds to PI(3,4)P2. Accordingly, the structures of the PLCδ and pleckstrin PH domains are not suitable templates for modeling the Akt PH domain, because their phospholipid-binding specificity is different from that of the Akt PH domain. As explained above, the structure of the BTK PH domain was selected as our template in modeling the Akt PH domain. Thus, our model of the Akt PH domain can reasonably explain the specificity of the Akt PH domain for PI(3,4)P2.

Estimated Binding Affinities. Both the SCORE[76] and ChemScore[77] methods use an empirical scoring function to estimate the binding free energy for a protein−ligand complex when the 3D structure of the complex is known. The scoring function of SCORE contains terms to estimate van der Waals contacts, metal−ligand bonding, hydrogen bonding, desolvation effects, and a deformation penalty upon binding. In comparison, the scoring function of ChemScore uses similar terms except for a desolvation term to predict the binding free energy of the protein−ligand complex. The training datasets used in these two methods include a large number of divergent protein−ligand complexes (SCORE: 170 protein−ligand complexes; ChemScore: 82 protein−ligand complexes). Most importantly, the scoring functions of SCORE and ChemScore successfully reproduced the binding affinities of the entire training set with a cross-validation deviation of 6.3 and 8.68 kJ/mol, respectively. Thus, we used these two methods to estimate the binding affinity of the Akt PH domain in complex with PI3-K-generated phospholipids. The estimated binding affinities are listed in Table 3.

Table 3. Estimated pK_d by SCORE and ChemScore

	estimated pK_d		experimental data		
compd	SCORE	ChemScore	K_d (μM)/ pK_d[a]	activity (%)[b]	IC_{50} (μM)/ pIC_{50}[c]
PI(3,4)P2	6.32	6.46	0.57/6.24	100	
PI(3,4,5)P3	6.11	6.43	0.40/6.40	−35	
PI(3)P	4.13	5.03		13	
1	4.43	5.26			5.0/5.30
2	4.12	4.84			32.0/4.49

[a] Ref 11. [b] Ref 10. [c] Ref 92.

Chart 2

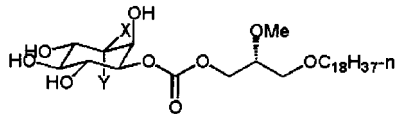

1 X = H, Y = CH_2OH
2 X= CH_2OH, Y = H

The predicted binding affinities based on the complex models reveal that PI(3,4)P2 and PI(3,4,5)P3 have comparable dissociation constants, which is consistent with the experimental fact that the Akt PH domain binds almost equally well both PI(3,4)P2 and PI(3,4,5)-P3.[10,11,91] It is worth noting that the estimated dissociation constants of PI(3,4)P2 and PI(3,4,5)P3 are approximately the same as those determined experimentally (Table 3). In addition, the estimated binding affinity of PI(3)P is 10−100-fold less than those of PI(3,4)P2 and PI(3,4,5)P3, which is consistent with the experimental measurement.[10,11,91] The correct prediction of the relative and absolute binding affinities of PI(3)P, PI(3,4)-P2, and PI(3,4,5)P3 for the Akt PH domain provides further support for our 3D structural model of this PH domain.

Application of the Model of the Akt PH Domain. The 3D structural model of the Akt PH domain has been used to examine the interaction and binding affinity of 3-(hydroxymethyl)-bearing phosphatidylinositol ether lipid analogues bound to the Akt PH domain.[92]

The 3D structural models of the Akt PH domain in complex with the synthesized Akt ligands **1** and **2** (Chart 2) were achieved through the FlexX docking process followed by energy minimization with a 10 Å water sphere, based upon which the binding affinities were estimated by the empirical scoring functions SCORE and ChemScore.

The predicted binding affinities of compounds **1** and **2** in complex with the Akt PH domain are presented in

Table 3. Although the estimated binding affinities by SCORE and ChemScore are different, both methods predicted that compound **1** should be more active than compound **2**. The binding affinities predicted by ChemScore are in line with the experimental results (Table 3). This result again provides support for our model of the Akt PH domain and suggests that the model can be used for structure-based design of Akt ligands to modify Akt activity.

The differences in the activities of compounds **1** and **2** can be accounted for based upon their hydrogen bond interactions with the Akt PH domain. These models show that the majority of the hydrogen bond interactions formed between compounds **1** and **2** in their complexes with the Akt PH domain are similar. Differences occur only at the 3-hydroxymethyl group. The 3-hydroxymethyl group which is axially oriented in compound **1** interacts with Arg25 through two hydrogen bonds, whereas the equatorial 3-hydroxymethyl group in compound **2** is situated so as to be unable to form a hydrogen bond with Arg25. In addition, the different orientation of the 3-hydroxymethyl group of compounds **1** and **2** results in the different location of compounds **1** and **2** within the binding pocket of the Akt PH domain so that the 1-carbonate group of compound **1** forms two hydrogen bonds with Arg23, while that of compound **2** forms only one hydrogen bond with Arg23.

Summary

Homology modeling and docking simulations were performed to explore the structure of the Akt PH domain and its interaction with PI3-K-generated phospholipids. The PI3-K-generated phospholipids bind to the positively charged residues situated at the positively charged phospholipid-binding pocket formed by the $\beta1-\beta2$, $\beta3-\beta4$, and $\beta6-\beta7$ loops of the Akt PH domain. The shorter $\beta1-\beta2$ loop contributes to the inability of the Akt PH domain to accommodate the 5-phosphate group of a phospholipid, whereas the residues situated at the bottom of binding pocket, Lys14, Arg25, Tyr38, Arg48, and Arg86, can interact with the 3- and 4-phosphate groups of the PI3-K-generated phospholipids. The predicted binding mode is supported by results obtained by others from site-directed mutagenesis studies. Furthermore, the estimated binding affinities of PI3-K-generated phospholipids to the Akt PH domain using the modeled complexes are consistent with the experimental data. Finally, this model has been successfully used to rationalize differences in structure and Akt inhibitory activity between newly synthesized 3-hydroxymethyl-containing phosphatidylinositol ether lipid analogues. Taken together, our molecular modeling studies provide new insights into the binding of the Akt PH domain to its ligands, thus suggesting that this model may prove useful in further structure-based drug design.

Acknowledgment. This work was supported by the National Institutes of Health (Grant No. CA61015), by the Department of Defense (DAMD 17-93-V-3018), and in part by the Office of Naval Research.

References

(1) Franke, T. F.; Yang, S. I.; Chan, T. O.; Datta, K.; Kazlauskas, A.; Morrison, D. K.; Kaplan, D. R.; Tsichlis, P. N. The protein kinase encoded by the Akt proto-oncogene is a target of the PDGF-activated phosphatidylinositol 3-kinase. *Cell* **1995**, *81*, 727−736.

(2) Andjelkovic, M.; Jakubowicz, T.; Cron, P.; Ming, X. F.; Han, J. W.; Hemmings, B. A. Activation and phosphorylation of a pleckstrin homology domain containing protein kinase (RAC-PK/PKB) promoted by serum and protein phosphatase inhibitors. *Proc. Natl. Acad. Sci. U.S.A.* **1996**, *93*, 5699−5704.

(3) Klippel, A.; Reinhard, C.; Kavanaugh, W. M.; Apell, G.; Escobedo, M. A.; Williams, L. T. Membrane localization of phosphatidylinositol 3-kinase is sufficient to activate multiple signal-transducing kinase pathways. *Mol. Cell Biol.* **1996**, *16*, 4117−4127.

(4) Datta, K.; Bellacosa, A.; Chan, T. O.; Tsichlis, P. N. Akt is a direct target of the phosphatidylinositol 3-kinase. Activation by growth factors, v-src and v-Ha-ras, in Sf9 and mammalian cells. *J. Biol. Chem.* **1996**, *271*, 30835−30839.

(5) Auger, K. R.; Serunian, L. A.; Soltoff, S. P.; Libby, P.; Cantley, L. C. PDGF-dependent tyrosine phosphorylation stimulates production of novel polyphosphoinositides in intact cells. *Cell* **1989**, *57*, 167−175.

(6) Carpenter, C. L.; Duckworth, B. C.; Auger, K. R.; Cohen, B.; Schaffhausen, B. S.; Cantley, L. C. Purification and characterization of phosphoinositide 3-kinase from rat liver. *J. Biol. Chem.* **1990**, *265*, 19704−19711.

(7) Burgering, B. M.; Coffer, P. J. Protein kinase B (c-Akt) in phosphatidylinositol-3-OH kinase signal transduction. *Nature* **1995**, *376*, 599−602.

(8) Park, E. K.; Yang, S. I.; Kang, S. S. Activation of Akt by nerve growth factor via phosphatidylinositol-3 kinase in PC12 pheochromocytoma cells. *Mol. Cells* **1996**, *6*, 494−498.

(9) James, S. R.; Downes, C. P.; Gigg, R.; Grove, S. J.; Holmes, A. B.; Alessi, D. R. Specific binding of the Akt-1 protein kinase to phosphatidylinositol 3,4,5-trisphosphate without subsequent activation. *Biochem. J.* **1996**, *315*, 709−713.

(10) Franke, T. F.; Kaplan, D. R.; Cantley, L. C.; Toker, A. Direct regulation of the Akt proto-oncogene product by phosphatidylinositol-3,4-bisphosphate. *Science* **1997**, *275*, 665−668.

(11) Frech, M.; Andjelkovic, M.; Ingley, E.; Reddy, K. K.; Falck, J. R.; Hemmings, B. A. High affinity binding of inositol phosphates and phosphoinositides to the pleckstrin homology domain of RAC/protein kinase B and their influence on kinase activity. *J. Biol. Chem.* **1997**, *272*, 8474−8481.

(12) Downward, J. Lipid-regulated kinases: some common themes at last. *Science* **1998**, *279*, 673−674.

(13) Currie, R. A.; Walker, K. S.; Gray, A.; Deak, M.; Casamayor, A.; Downes, C. P.; Cohen, P.; Alessi, D. R.; Lucocq, J. Role of phosphatidylinositol 3,4,5-trisphosphate in regulating the activity and localization of 3-phosphoinositide-dependent protein kinase-1. *Biochem. J.* **1999**, *337*, 575−583.

(14) Sable, C. L.; Filippa, N.; Filloux, C.; Hemmings, B. A.; Van Obberghen, E. Involvement of the pleckstrin homology domain in the insulin-stimulated activation of protein kinase B. *J. Biol. Chem.* **1998**, *273*, 29600−29606.

(15) Zhang, X.; Vik, T. A. Growth factor stimulation of hematopoietic cells leads to membrane translocation of AKT1 protein kinase. *Leuk. Res.* **1997**, *21*, 849−856.

(16) Wijkander, J.; Holst, L. S.; Rahn, T.; Resjo, S.; Castan, I.; Manganiello, V.; Belfrage, P.; Degerman, E. Regulation of protein kinase B in rat adipocytes by insulin, vanadate, and peroxovanadate. Membrane translocation in response to peroxovanadate. *J. Biol. Chem.* **1997**, *272*, 21520−21526.

(17) Meier, R.; Alessi, D. R.; Cron, P.; Andjelkovic, M.; Hemmings, B. A. Mitogenic activation, phosphorylation, and nuclear translocation of protein kinase Bbeta. *J. Biol. Chem.* **1997**, *272*, 30491−30497.

(18) Andjelkovic, M.; Alessi, D. R.; Meier, R.; Fernandez, A.; Lamb, N. J.; Frech, M.; Cron, P.; Cohen, P.; Lucocq, J. M.; Hemmings, B. A. Role of translocation in the activation and function of protein kinase B. *J. Biol. Chem.* **1997**, *272*, 31515−31524.

(19) Soskic, V.; Gorlach, M.; Poznanovic, S.; Boehmer, F. D.; Godovac-Zimmermann, J. Functional proteomics analysis of signal transduction pathways of the platelet-derived growth factor beta receptor. *Biochemistry* **1999**, *38*, 1757−1764.

(20) Alessi, D. R.; Deak, M.; Casamayor, A.; Caudwell, F. B.; Morrice, N.; Norman, D. G.; Gaffney, P.; Reese, C. B.; MacDougall, C. N.; Harbison, D.; Ashworth, A.; Bownes, M. 3-Phosphoinositide-dependent protein kinase-1 (PDK1): structural and functional homology with the Drosophila DSTPK61 kinase. *Curr. Biol.* **1997**, *7*, 776−789.

(21) Stephens, L.; Anderson, K.; Stokoe, D.; Erdjument-Bromage, H.; Painter, G. F.; Holmes, A. B.; Gaffney, P. R.; Reese, C. B.; McCormick, F.; Tempst, P.; Coadwell, J.; Hawkins, P. T. Protein kinase B kinases that mediate phosphatidylinositol 3,4,5-trisphosphate-dependent activation of protein kinase B. *Science* **1998**, *279*, 710−714.

(22) Kohn, A. D.; Takeuchi, F.; Roth, R. A. Akt, a pleckstrin homology domain containing kinase, is activated primarily by phosphorylation. *J. Biol. Chem.* **1996**, *271*, 21920−21926.
(23) Stokoe, D.; Stephens, L. R.; Copeland, T.; Gaffney, P. R.; Reese, C. B.; Painter, G. F.; Holmes, A. B.; McCormick, F.; Hawkins, P. T. Dual role of phosphatidylinositol-3,4,5-trisphosphate in the activation of protein kinase B. *Science* **1997**, *277*, 567−570.
(24) Maehama, T.; Dixon, J. E. The tumor suppressor, PTEN/MMAC1, dephosphorylates the lipid second messenger, phosphatidylinositol 3,4,5-trisphosphate. *J. Biol. Chem.* **1998**, *273*, 13375−13378.
(25) Li, J.; Yen, C.; Liaw, D.; Podsypanina, K.; Bose, S.; Wang, S. I.; Puc, J.; Miliaresis, C.; Rodgers, L.; McCombie, R.; Bigner, S. H.; Giovanella, B. C.; Ittmann, M.; Tycko, B.; Hibshoosh, H.; Wigler, M. H.; Parsons, R. PTEN, a putative protein tyrosine phosphatase gene mutated in human brain, breast, and prostate cancer. *Science* **1997**, *275*, 1943−1947.
(26) Steck, P. A.; Pershouse, M. A.; Jasser, S. A.; Yung, W. K.; Lin, H.; Ligon, A. H.; Langford, L. A.; Baumgard, M. L.; Hattier, T.; Davis, T.; Frye, C.; Hu, R.; Swedlund, B.; Teng, D. H.; Tavtigian, S. V. Identification of a candidate tumour suppressor gene, MMAC1, at chromosome 10q23.3 that is mutated in multiple advanced cancers. *Nat. Genet.* **1997**, *15*, 356−362.
(27) Stambolic, V.; Suzuki, A.; de la Pompa, J. L.; Brothers, G. M.; Mirtsos, C.; Sasaki, T.; Ruland, J.; Penninger, J. M.; Siderovski, D. P.; Mak, T. W. Negative regulation of PKB/Akt-dependent cell survival by the tumor suppressor PTEN. *Cell* **1998**, *95*, 29−39.
(28) Datta, S. R.; Dudek, H.; Tao, X.; Masters, S.; Fu, H.; Gotoh, Y.; Greenberg, M. E. Akt phosphorylation of BAD couples survival signals to the cell-intrinsic death machinery. *Cell* **1997**, *91*, 231−241.
(29) del Peso, L.; Gonzalez-Garcia, M.; Page, C.; Herrera, R.; Nunez, G. Interleukin-3-induced phosphorylation of BAD through the protein kinase Akt. *Science* **1997**, *278*, 687−689.
(30) Cardone, M. H.; Roy, N.; Stennicke, H. R.; Salvesen, G. S.; Franke, T. F.; Stanbridge, E.; Frisch, S.; Reed, J. C. Regulation of cell death protease caspase-9 by phosphorylation [see comments]. *Science* **1998**, *282*, 1318−1321.
(31) Cross, D. A.; Alessi, D. R.; Cohen, P.; Andjelkovich, M.; Hemmings, B. A. Inhibition of glycogen synthase kinase-3 by insulin mediated by protein kinase B. *Nature* **1995**, *378*, 785−789.
(32) Shaw, M.; Cohen, P.; Alessi, D. R. Further evidence that the inhibition of glycogen synthase kinase-3beta by IGF-1 is mediated by PDK1/PKB-induced phosphorylation of Ser-9 and not by dephosphorylation of Tyr-216. *FEBS Lett.* **1997**, *416*, 307−311.
(33) Staveley, B. E.; Ruel, L.; Jin, J.; Stambolic, V.; Mastronardi, F. G.; Heitzler, P.; Woodgett, J. R.; Manoukian, A. S. Genetic analysis of protein kinase B (AKT) in Drosophila. *Curr. Biol.* **1998**, *8*, 599−602.
(34) Yao, R.; Cooper, G. M. Requirement for phosphatidylinositol-3 kinase in the prevention of apoptosis by nerve growth factor. *Science* **1995**, *267*, 2003−2006.
(35) Yao, R.; Cooper, G. M. Growth factor-dependent survival of rodent fibroblasts requires phosphatidylinositol 3-kinase but is independent of pp70S6K activity. *Oncogene* **1996**, *13*, 343−351.
(36) Basu, S.; Kolesnick, R. Stress signals for apoptosis: ceramide and c-Jun kinase. *Oncogene* **1998**, *17*, 3277−3285.
(37) Zhou, H.; Summers, S. A.; Birnbaum, M. J.; Pittman, R. N. Inhibition of Akt kinase by cell-permeable ceramide and its implications for ceramide-induced apoptosis. *J. Biol. Chem.* **1998**, *273*, 16568−16575.
(38) Summers, S. A.; Garza, L. A.; Zhou, H.; Birnbaum, M. J. Regulation of insulin-stimulated glucose transporter GLUT4 translocation and Akt kinase activity by ceramide. *Mol. Cell Biol.* **1998**, *18*, 5457−5464.
(39) Zundel, W.; Giaccia, A. Inhibition of the anti-apoptotic PI(3)K/Akt/Bad pathway by stress. *Genes Dev.* **1998**, *12*, 1941−1946.
(40) Philpott, K. L.; McCarthy, M. J.; Klippel, A.; Rubin, L. L. Activated phosphatidylinositol 3-kinase and Akt kinase promote survival of superior cervical neurons. *J. Cell Biol.* **1997**, *139*, 809−815.
(41) Gibson, T. J.; Hyvonen, M.; Musacchio, A.; Saraste, M.; Birney, E. PH domain: the first anniversary. *Trends Biochem. Sci.* **1994**, *19*, 349−353.
(42) Lemmon, M. A.; Ferguson, K. M.; Schlessinger, J. PH domains: diverse sequences with a common fold recruit signaling molecules to the cell surface. *Cell* **1996**, *85*, 621−624.
(43) Rebecchi, M. J.; Scarlata, S. Pleckstrin homology domains: a common fold with diverse functions. *Annu. Rev. Biophys. Biomol. Struct.* **1998**, *27*, 503−528.
(44) Lemmon, M. A.; Falasca, M.; Ferguson, K. M.; Schlessinger, J. Regulatory reruitment of signaling molecules to the cell membrane by pleckstrin homology domains. *Trends Cell Biol.* **1997**, *7*, 237−242.
(45) Cifuentes, M. E.; Honkanen, L.; Rebecchi, M. J. Proteolytic fragments of phosphoinositide-specific phospholipase C-delta 1. Catalytic and membrane binding properties. *J. Biol. Chem.* **1993**, *268*, 11586−11593.
(46) Cifuentes, M. E.; Delaney, T.; Rebecchi, M. J. D-myo-inositol 1,4,5-trisphosphate inhibits binding of phospholipase C-delta 1 to bilayer membranes. *J. Biol. Chem.* **1994**, *269*, 1945−1948.
(47) Fukuda, M.; Kojima, T.; Kabayama, H.; Mikoshiba, K. Mutation of the pleckstrin homology domain of Bruton's tyrosine kinase in immunodeficiency impaired inositol 1,3,4,5-tetrakisphosphate binding capacity. *J. Biol. Chem.* **1996**, *271*, 30303−30306.
(48) Kojima, T.; Fukuda, M.; Watanabe, Y.; Hamazato, F.; Mikoshiba, K. Characterization of the pleckstrin homology domain of Btk as an inositol polyphosphate and phosphoinositide binding domain. *Biochem. Biophys. Res. Commun.* **1997**, *236*, 333−339.
(49) Scharenberg, A. M.; El-Hillal, O.; Fruman, D. A.; Beitz, L. O.; Li, Z.; Lin, S.; Gout, I.; Cantley, L. C.; Rawlings, D. J.; Kinet, J. P. Phosphatidylinositol-3,4,5-trisphosphate (PtdIns-3,4,5-P3)/Tec kinase- dependent calcium signaling pathway: a target for SHIP-mediated inhibitory signals. *EMBO J.* **1998**, *17*, 1961−1972.
(50) Klippel, A.; Kavanaugh, W. M.; Pot, D.; Williams, L. T. A specific product of phosphatidylinositol 3-kinase directly activates the protein kinase Akt through its pleckstrin homology domain. *Mol. Cell Biol.* **1997**, *17*, 338−344.
(51) Nilges, M.; Macias, M. J.; O'Donoghue, S. I.; Oschkinat, H. Automated NOESY interpretation with ambiguous distance restraints: the refined NMR solution structure of the pleckstrin homology domain from beta-spectrin. *J. Mol. Biol.* **1997**, *269*, 408−422.
(52) Yoon, H. S.; Hajduk, P. J.; Petros, A. M.; Olejniczak, E. T.; Meadows, R. P.; Fesik, S. W. Solution structure of a pleckstrin-homology domain. *Nature* **1994**, *369*, 672−675.
(53) Timm, D.; Salim, K.; Gout, I.; Guruprasad, L.; Waterfield, M.; Blundell, T. Crystal structure of the pleckstrin homology domain from dynamin. *Nat. Struct. Biol.* **1994**, *1*, 782−788.
(54) Ferguson, K. M.; Lemmon, M. A.; Schlessinger, J.; Sigler, P. B. Structure of the high affinity complex of inositol trisphosphate with a phospholipase C pleckstrin homology domain. *Cell* **1995**, *83*, 1037−1046.
(55) Hyvonen, M.; Saraste, M. Structure of the PH domain and Btk motif from Bruton's tyrosine kinase: molecular explanations for X-linked agammaglobulinaemia. *EMBO J.* **1997**, *16*, 3396−3404.
(56) Sonnhammer, E. L.; Eddy, S. R.; Durbin, R. Pfam: a comprehensive database of protein domain families based on seed alignments. *Proteins* **1997**, *28*, 405−420.
(57) Sonnhammer, E. L.; Eddy, S. R.; Birney, E.; Bateman, A.; Durbin, R. Pfam: multiple sequence alignments and HMM-profiles of protein domains. *Nucleic Acids Res.* **1998**, *26*, 320−322.
(58) Bateman, A.; Birney, E.; Durbin, R.; Eddy, S. R.; Finn, R. D.; Sonnhammer, E. L. Pfam 3.1: 1313 multiple alignments and profile HMMs match the majority of proteins. *Nucleic Acids Res.* **1999**, *27*, 260−262.
(59) Cuff, J. A.; Clamp, M. E.; Siddiqui, A. S.; Finlay, M.; Barton, G. J. JPred: a consensus secondary structure prediction server. *Bioinformatics* **1998**, *14*, 892−893.
(60) Cuff, J. A.; Barton, G. J. Evaluation and improvement of multiple sequence methods for protein secondary structure prediction. *Proteins* **1999**, *34*, 508−519.
(61) Laskowski, R. A.; Hutchinson, E. G.; Michie, A. D.; Wallace, A. C.; Jones, M. L.; Thornton, J. M. PDBsum: a Web-based database of summaries and analyses of all PDB structures. *Trends Biochem. Sci.* **1997**, *22*, 488−490.
(62) Holm, L.; Sander, C. Mapping the protein universe. *Science* **1996**, *273*, 595−603.
(63) Holm, L.; Sander, C. Alignment of three-dimensional protein structures: network server for database searching. *Methods Enzymol.* **1996**, *266*, 653−662.
(64) Baraldi, E.; Carugo, K. D.; Hyvonen, M.; Surdo, P. L.; Riley, A. M.; Potter, B. V.; O'Brien, R.; Ladbury, J. E.; Saraste, M. Structure of the PH domain from Bruton's tyrosine kinase in complex with inositol 1,3,4,5-tetrakisphosphate. *Struct. Fold. Des.* **1999**, *7*, 449−460.
(65) Hobohm, U.; Scharf, M.; Schneider, R.; Sander, C. Selection of representative protein data sets. *Protein Sci.* **1992**, *1*, 409−417.
(66) Hobohm, U.; Sander, C. Enlarged representative set of protein structures. *Protein Sci.* **1994**, *3*, 522−524.
(67) Weiner, S. J.; Kollman, P. A.; Case, D. A.; Singh, U. C.; Ghio, C.; Alagona, G.; Profeta, S. J.; Weiner, P. A new force field for molecular mechanical simulation of nucleic acids and proteins. *J. Am. Chem. Soc.* **1984**, *106*, 765−784.
(68) Weiner, S. J.; Kollman, P. A.; Nguyen, D. T.; Case, D. A. An all atom force field for simulations of proteins and nucleic acid. *J. Comput. Chem.* **1986**, *7*, 230−252.
(69) Rodriguez, R.; Chinea, G.; Lopez, N.; Pons, T.; Vriend, G. Homology modeling, model and software evaluation: three related resources. *Bioinformatics* **1998**, *14*, 523−528.

(70) Rarey, M.; Kramer, B.; Lengauer, T.; Klebe, G. A fast flexible docking method using an incremental construction algorithm. *J. Mol. Biol.* **1996**, *261*, 470−489.
(71) Berman, H. M.; Westbrook, J.; Feng, Z.; Gilliland, G.; Bhat, T. N.; Weissig, H.; Shindyalov, I. N.; Bourne, P. E. The Protein Data Bank. *Nucleic Acids Res.* **2000**, *28*, 235−242.
(72) Brooks, B. R.; Bruccoleri, R. E.; Olafson, B. D.; States, D. J.; Swaminathan, S.; Karplus, M. CHARMM: A program for macromolecular energy, minimization, and dynamics calculations. *J. Comput. Chem.* **1983**, *4*, 187−217.
(73) MacKerell, A. D.; Wiorkiewicz-Kuczera, J. J.; Karplus, M. An all-atom empirical energy function for the simulation of nucleic acids. *J. Am. Chem. Soc.* **1995**, *117*, 11946−11975.
(74) MacKerell, A. D.; Bashford, J. D.; Bellott, M.; Dunbrack Jr, R. L.; Evanseck, J. D.; Field, M. J.; Fischer, S.; Gao, J.; Guo, H.; Ha, S.; Joseph-McCarthy, D.; Kuchnir, L.; Kuczera, K.; Lau, F. T. K.; Mattos, C.; Michnick, S.; Ngo, T.; Nguyen, D. T.; Prodhom, B.; Reiher, W. E.; Roux, B.; Schlenkrich, M.; Smith, J. C.; Stote, R.; Straub, J.; Watanabe, M.; Wiorkiewicz-Kuczera, J.; Yin, D.; Karplus, M. All-atom empirical potential for molecular modeling and dynamics studies of proteins. *J. Phys. Chem.* **1998**, *102*, 3586−3616.
(75) van Gunsteren, W. F.; Berendsen, H. J. C. Algorithms for macromolecular dynamics and constraint dynamics. *Mol. Phys.* **1977**, *34*, 1311−1327.
(76) Wang, R. X.; Liu, L.; Lai, L. H.; Tang, Y. Q. SCORE: A new empirical method for estimating the binding affinity of a protein−ligand complex. *J. Mol. Model.* **1998**, *4*, 379−394.
(77) Bldridge, M. D.; Murray, C. W.; Auton, T. R.; Paolini, G. V.; Mee, R. P. Empirical scoring function: I. The development of a fast empirical scoring function to estimate the binding affinity of ligands in receptor complexes. *J. Comput.-Aided Mol. Des.* **1997**, *11*, 425−445.
(78) Smith, R. F.; Wiese, B. A.; Wojzynski, M. K.; Davison, D. B.; Worley, K. C. BCM Search Launcher−an integrated interface to molecular biology database search and analysis services available on the World Wide Web. *Genome Res.* **1996**, *6*, 454−462.
(79) Worley, K. C.; Wiese, B. A.; Smith, R. F. BEAUTY: an enhanced BLAST-based search tool that integrates multiple biological information resources into sequence similarity search results. *Genome Res.* **1995**, *5*, 173−184.
(80) Jeanmougin, F.; Thompson, J. D.; Gouy, M.; Higgins, D. G.; Gibson, T. J. Multiple sequence alignment with Clustal X. *Trends Biochem. Sci.* **1998**, *23*, 403−405.
(81) Thompson, J. D.; Higgins, D. G.; Gibson, T. J. CLUSTAL W: improving the sensitivity of progressive multiple sequence alignment through sequence weighting, position-specific gap penalties and weight matrix choice. *Nucleic Acids Res.* **1994**, *22*, 4673−4680.
(82) Altschul, S. F.; Madden, T. L.; Schaffer, A. A.; Zhang, J.; Zhang, Z.; Miller, W.; Lipman, D. J. Gapped BLAST and PSI−BLAST: a new generation of protein database search programs. *Nucleic Acids Res.* **1997**, *25*, 3389−3402.
(83) Bellacosa, A.; Chan, T. O.; Ahmed, N. N.; Datta, K.; Malstrom, S.; Stokoe, D.; McCormick, F.; Feng, J.; Tsichlis, P. Akt activation by growth factors is a multiple-step process: the role of the PH domain. *Oncogene* **1998**, *17*, 313−325.
(84) Vihinen, M.; Brandau, O.; Branden, L. J.; Kwan, S. P.; Lappalainen, I.; Lester, T.; Noordzij, J. G.; Ochs, H. D.; Ollila, J.; Pienaar, S. M.; Riikonen, P.; Saha, B. K.; Smith, C. I. E. BTKbase, mutation database for X-linked agammaglobulinemia (XLA). *Nucleic Acids Res.* **1998**, *26*, 242−247.
(85) Bromann, P. A.; Boetticher, E. E.; Lomasney, J. W. A single amino acid substitution in the pleckstrin homology domain of phospholipase C delta1 enhances the rate of substrate hydrolysis. *J. Biol. Chem.* **1997**, *272*, 16240−16246.
(86) Klein, D. E.; Lee, A.; Frank, D. W.; Marks, M. S.; Lemmon, M. A. The pleckstrin homology domains of dynamin isoforms require oligomerization for high affinity phosphoinositide binding. *J. Biol. Chem.* **1998**, *273*, 27725−27733.
(87) Hurley, J. H.; Misra, S. Signaling and subcellular targeting by membrane-binding domains. *Annu. Rev. Biophys. Biomol. Struct.* **2000**, *29*, 49−79.
(88) Li, T.; Rawlings, D. J.; Park, H.; Kato, R. M.; Witte, O. N.; Satterthwaite, A. B. Constitutive membrane association potentiates activation of Bruton tyrosine kinase. *Oncogene* **1997**, *15*, 1375−1383.
(89) Rebecchi, M.; Peterson, A.; McLaughlin, S. Phosphoinositide-specific phospholipase C-delta 1 binds with high affinity to phospholipid vesicles containing phosphatidylinositol 4,5-bisphosphate. *Biochemistry* **1992**, *31*, 12742−12747.
(90) Harlan, J. E.; Hajduk, P. J.; Yoon, H. S.; Fesik, S. W. Pleckstrin homology domains bind to phosphatidylinositol-4,5- bisphosphate. *Nature* **1994**, *371*, 168−170.
(91) Kavran, J. M.; Klein, D. E.; Lee, A.; Falasca, M.; Isakoff, S. J.; Skolnik, E. Y.; Lemmon, M. A. Specificity and promiscuity in phosphoinositide binding by pleckstrin homology domains. *J. Biol. Chem.* **1998**, *273*, 30497−30508.
(92) Hu, Y. H.; Qiao, L. X.; Wang, S. M.; Rong, S. B.; Meuillet, E. J.; Berggren, M.; Gallegos, A.; Powis, G.; Kozikowski, A. P. The 3-(hydroxymethyl)-D-myo-inositol ether lipid phosphates and carbonates as inhibitors of the phosphatidylinositol 3-kinase signaling pathway. *J. Med. Chem.* **2000**, *43*, 3045−3051.

JM000493I